JACS
JOURNAL OF THE AMERICAN CHEMICAL SOCIETY
Article
pubs.acs.org/JACS

Volatile Single-Source Precursors for the Low-Temperature Preparation of Sodium–Rare Earth Metal Fluorides

Matthew C. Barry, Zheng Wei, Tianyu He, Alexander S. Filatov, and Evgeny V. Dikarev*

Department of Chemistry, University at Albany, SUNY, Albany, New York 12222, United States

Supporting Information

ABSTRACT: Heterometallic single-source precursors for the preparation of sodium–rare earth metal fluorides are reported. Fluorinated β-diketonates NaRE(hfac)$_4$ (RE = Y (**1**), Er (**2**), and Eu (**3**); hfac = hexafluoroacetylacetonate) have been obtained on a large scale, in high yield, via one-pot reaction that utilizes commercially available starting reagents. The solid-state structures of the title complexes consist of 1D polymeric chains with alternating [Na] and [RE(hfac)$_4$] units. Compounds **1**–**3** are highly volatile and exhibit a fair stability in open air. Mass spectrometric investigation indicates the presence of heterometallic fragments in the gas phase. The presence of heterometallic species in solutions of coordinating solvents has also been confirmed. Decomposition of heterometallic precursors in argon atmosphere was shown to yield phase-pure sodium–rare earth metal fluorides. Low decomposition temperature effectively allows for a high degree of control over the formation of both kinetic α-phases and thermodynamic β-phases of target NaREF$_4$ (RE = Y, Er, and Eu) materials.

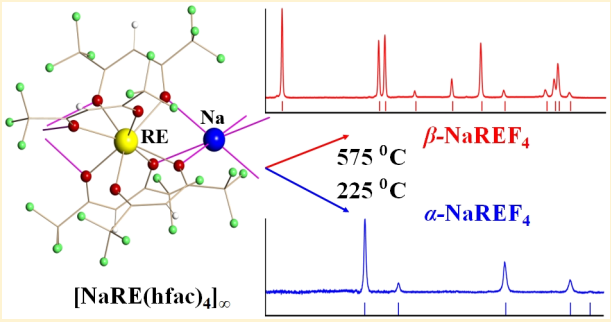

INTRODUCTION

When considering up- and down-conversion materials[1] for specific applications, the host lattice[2] as well as dopant nature[3] and concentrations[4] should be taken into account.[5] It is well established[6] that the alkali–rare earth metal fluorides, AREF$_4$, are among the most effective conversion materials. Of those materials, NaYF$_4$ is currently regarded[7] to be the best suited for a host lattice, while the lanthanide metals such as Er and Eu have been incorporated[8] as highly efficient dopants that enable the absorption of a wide range of the electromagnetic spectrum. The NaREF$_4$ compounds are known[9] to exist in two polymorph modifications: kinetic cubic (α) phase and thermodynamic hexagonal (β) phase that afford a different control of dopants within the matrix,[10] which is crucial for various applications.

Research into NaREF$_4$ materials has been primarily focused on obtaining phase-pure[9c] products that are single-crystalline[11] and monodisperse.[12] Several multi-source precursor approaches have been suggested, including thermal decomposition,[13] hydro(solvo)thermal routes,[14] co-precipitation,[15] and ionic liquids-based synthesis.[16] Sol–gel methods, in particular, are some of the most commonly reported[17] techniques for the growth of NaREF$_4$ thin films. Practical applications of these methods revealed that the experimental variables such as pressure,[18] temperature,[19] and reaction time[20] all have a profound impact on the final product properties.[21] Harsh reaction conditions can make it difficult to control the purity, size, and shape of target particles and thin films.[22]

In order to expand the range of practical applications of NaREF$_4$ fluorides, the methods of *soft chemistry* approach that utilize low temperatures and pressures as well as safer starting reagents are needed.[23] Single-source precursors can provide precise control over material stoichiometry at the molecular level and offer kinetically attractive decomposition routes for the preparation of fine particles. While low-temperature thermolysis will ensure the formation of specific phase-pure polymorph modification, carrying out the preparation at ambient pressure will limit the appearance of impurities.[17] A single-source precursor approach for the preparation of NaREF$_4$ materials has been recently introduced by Mishra et al.,[24] who synthesized a number of heterometallic Na-RE trifluoroacetate adducts with THF and di-, tri-, and tetraglyme and decomposed those in high-boiling solvents to successfully isolate fluoride materials.

Herein we report isolation, characterization, and decomposition study of the first volatile heterometallic single-source precursors NaRE(hfac)$_4$ (RE = Y (**1**), Er (**2**), and Eu (**3**)) with a proper 1:1 metal ratio. Low-temperature decomposition of the title fluorinated β-diketonates was shown to afford phase-pure α- and β-modifications of the target NaREF$_4$ fluorides.

RESULTS AND DISCUSSION

Heterometallic fluorinated β-diketonates NaRE(hfac)$_4$ (RE = Y (**1**), Er (**2**), and Eu (**3**); hfac = hexafluoroacetylacetonate) were initially obtained by the solid-state stoichiometric reaction (1) between the corresponding homometallic diketonates:

Received: April 24, 2016
Published: May 27, 2016

DOI: 10.1021/jacs.6b04194
J. Am. Chem. Soc. 2016, 138, 8883–8887

$$Na(hfac) + RE(hfac)_3 \rightarrow NaRE(hfac)_4 \quad (1)$$

While this reaction affords heterometallic compounds as a sole product, it requires prior preparation of unsolvated rare-earth hexafluoroacetylacetonates, which are extremely moisture-sensitive species. The above procedure was later improved by carrying out the interaction at 150−155 °C between commercially available reagents, Na(hfac) and anhydrous rare earth metal(III) chloride, taken in 4:1 ratio:

$$4Na(hfac) + RECl_3 \rightarrow NaRE(hfac)_3 + 3NaCl \quad (2)$$

Crystals of **1**−**3** can be readily collected with ca. 70−80% yield after 3 days in the cold end of a sealed ampule, while the nonvolatile second product, NaCl, remains in the hot zone of the container. The purity of products **1**−**3** has been confirmed by comparing their X-ray powder diffraction patterns with those calculated from the single crystal data (see Supporting Information (SI), Figures S1−S3 and Table S4). The procedure represented by reaction (2) can be effectively scaled up by running the reaction in solution at room temperature. Ethanol was originally implemented as a solvent; however, that requires the separation of the product from NaCl by sublimation under dynamic vacuum at 150 °C. Carrying out the reaction in acetone allows an efficient separation of the diketonates **1**−**3** from insoluble NaCl by filtration. Solid compounds can be obtained within hours in nearly quantitative yields by evaporation of the solvent under vacuum (SI, Tables S1−S3). The resulting products do not require any additional purification and are identical to those isolated by the solid-state technique (Figure 1). Heterometallic diketonates **1**−**3** were found to be relatively stable in moist air and can be handled without the use of a glovebox in a course of characterization and decomposition studies.

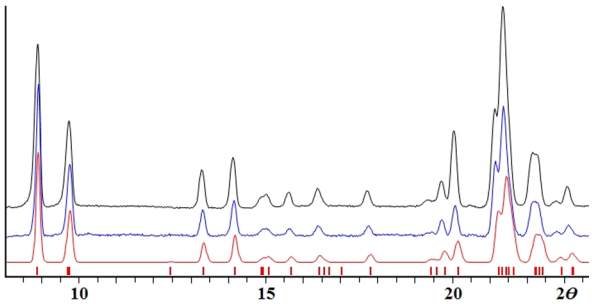

Figure 1. Comparison of X-ray powder diffraction patterns of heterometallic diketonate $NaY(hfac)_4$ (**1**) obtained by the solution (blue) and solid-state (black) methods with the theoretical pattern (red) calculated from the single-crystal data.

Elongated prismatic crystals of **1**−**3** suitable for X-ray structural investigation were grown by sublimation in evacuated ampules placed in tube furnace with a temperature gradient of 150−155 °C for 12 h. X-ray diffraction study revealed that heterometallic diketonates $NaRE(hfac)_4$ (**1**−**3**) are isomorphous and exhibit very close parameters of the monoclinic *C* unit cell (SI, Table S5). The structures are built of 1D polymeric chains with alternating [Na] and $[RE(hfac)_4]$ units (Figure 2 and SI, Figures S4−S6). The chain dimensions are nearly identical for **1**−**3**, as evident from the RE···Na separations (Table 1) that differ by ca. 0.05 Å. Rare earth metal atoms exhibit square antiprismatic geometry of eight oxygens from four chelating diketonate ligands. All ligands act in bridging-chelating mode with two of those through both O-ends and the other two through only one. A pair of distinctive C−H stretching frequencies for these types of hfac ligand can be found in the ATR-IR spectra of **1**−**3** (SI, Figures S13−S15). As expected, the RE−O bonds to oxygen atoms involved in bridging interactions to sodium are ca. 0.07 Å longer than to those that are pure chelating (Table 1). Sodium centers that bridge $[RE(hfac)_4]$ units exhibit a highly distorted octahedral coordination environment with the O−Na−O angles of 63.9−68.4°. In addition, there are six Na···F interactions of ca. 2.8−3.0 Å that are significantly shorter than the sum of the corresponding van der Waals radii.[25] The title compounds can be formulated as $\{Na^+[RE(hfac)_4]^-\}_\infty$ with the RE−O bond lengths supporting this assignment as they match well with those in known $[RE^{III}(hfac)_4]^-$ anionic fragments.[26]

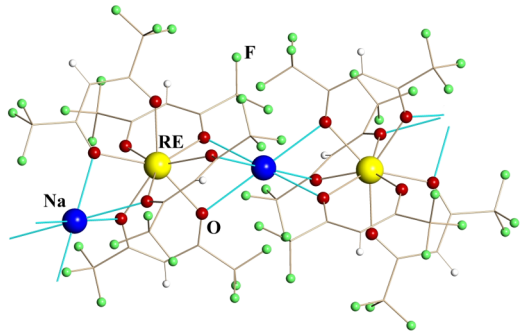

Figure 2. Fragment of the polymeric structure of $NaRE(hfac)_4$ (RE = Y (**1**), Er (**2**), and Eu (**3**)) drawn as ball-and-stick model. Sodium−oxygen bonds to diketonate ligands involved in bridging interactions are shown in blue. Full list of metal−oxygen distances as well as views of the structures **1**−**3** drawn with thermal ellipsoids can be found in the Supporting Information (Tables S7−S9 and Figures S4−S6).

Table 1. Average Distances (Å) in the Structures of Heterometallic Diketonates $NaRE(hfac)_4$ (1−3)

RE	RE−O_c[a]	RE−$O_{c\text{-}b}$[a]	Na−O	RE···Na	Na···F
Y (**1**)	2.28	2.35	2.59	3.72	2.90
Er (**2**)	2.28	2.35	2.59	3.71	2.87
Eu (**3**)	2.32	2.40	2.61	3.76	2.91

[a] c = chelating; c-b = chelating-bridging.

Heterometallic diketonates **1**−**3** are highly volatile in both static and dynamic vacuum and can be easily purified using "cold finger" at 150−160 °C for 3 h or by quantitative resublimation in an evacuated, sealed ampule at 150 °C for 24 h. Sublimation starts at ca. 130 °C, while the traces of decomposition become obvious at temperatures exceeding 200 °C. This provides a rather large ca. 70 °C temperature window between volatility and decomposition, a very important technological parameter in chemical vapor deposition application of precursors. It is worth noting that one of the possible dissociation fragments, Na(hfac), is not volatile until about 180 °C.

The composition of the species in the gas phase has been examined by mass spectrometry using DART (direct analysis in real time) ion source. Analysis of mass spectra of solid samples of **1**−**3** revealed a clear presence of heterometallic fragments in the gas phase (Figure 3). Positive mode is dominated by the $[M+Na]^+$ ions (M = $NaRE(hfac)_4$) with characteristic isotope distribution patterns (SI, Tables S10−S12 and Figures S7−S9).

DOI: 10.1021/jacs.6b04194
J. Am. Chem. Soc. 2016, 138, 8883−8887

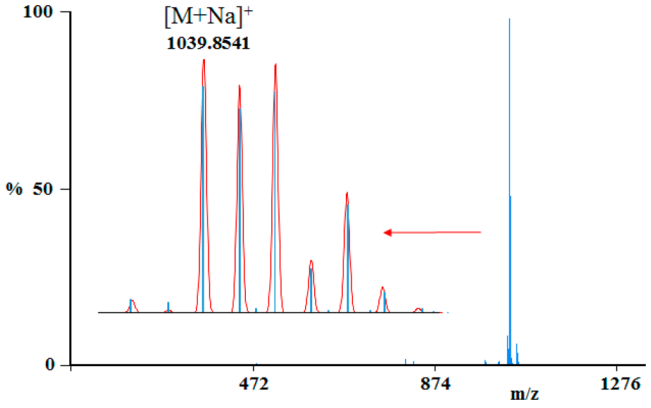

Figure 3. Positive-ion DART mass spectrum of solid $NaEr(hfac)_4$ (**2**). Isotope distribution pattern for the $[M+Na]^+$ peak (M = $NaEr(hfac)_4$) (blue) is compared with the calculated one (red).

High-nuclearity species $[M_2+Na]^+$ are also present, but much less abundant (0.3−1%).

Heterometallic diketonates **1**−**3** are readily soluble in common coordinating solvents (acetone, ethanol, THF, H_2O, DMSO), but are completely insoluble in non-coordinating ones (hexane, CH_2Cl_2, $CHCl_3$, benzene) in accord with their polymeric structures. It should be mentioned that $NaRE(hfac)_4$ compounds can be successfully recrystallized from solutions (SI, p S8) without yielding any adducts with coordinating solvents. Solution structure of diketonates **1**−**3** was examined in order to assess the retention of heterometallic species upon dissolution. NMR investigation of $NaY(hfac)_4$ (**1**) solution in acetone revealed a single peak in both ^1H and ^{19}F spectra that is clearly shifted relative to signals in the corresponding spectra of $Y(hfac)_3$ and Na(hfac) (Figure 4). As we have already shown[27] in a similar investigation of $Bi_2Zn(hfac)_8$ complex, the latter points to a presence of heterometallic species in solution and rules out possible dissociation of **1** into solvated homometallic fragments:

$$NaY(hfac)_4 + sol \rightarrow Na(hfac)(sol)_x + Y(hfac)_3(sol)_y \quad (3)$$

^1H and ^{19}F NMR spectra of both $NaEr(hfac)_4$ (**2**) and $NaEu(hfac)_4$ (**3**) are silent (SI, Figures S17 and S18), which also confirms the presence of heterometallic fragments in solutions of these compounds as it has been demonstrated before for a number of main group−transition metal diketonates.[28]

Mass-spectrometry investigation of heterometallic diketonates **1**−**3** dissolved in acetone using DART ion source concurs with the results of NMR study. Similar to the solid samples, the spectra obtained in the positive mode feature predominantly $[M+Na]^+$ ions (M = $NaRE(hfac)_4$) indicating the presence of heterometallic species in solution (SI, Tables S13−S15 and Figures S10−S12).

Thermal decomposition of $NaRE(hfac)_4$ (**1**−**3**) heterometallic precursors was carried out at various temperatures under an ambient pressure of argon using high alumina crucibles. All heterometallic compounds exhibit a low decomposition temperature at such conditions, and the appearance of target fluorides $NaREF_4$ can be detected by X-ray powder diffraction of residues at as low as 215 °C. Since the target fluorides $NaREF_4$ (RE = Y, Er, and Eu) are known to exist as two polymorph modifications, a great deal of effort was invested in determining the ideal conditions for isolation of both phases

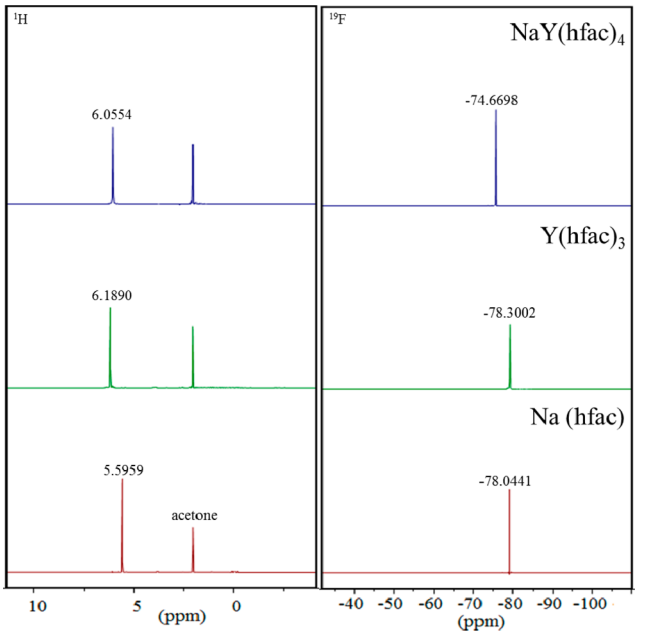

Figure 4. ^1H (left) and ^{19}F (right) NMR spectra of $NaY(hfac)_4$ (**1**) (blue), $Y(hfac)_3$ (green), and Na(hfac) (red) recorded in d^6-acetone at room temperature.

without any impurities in each case (Figure 5). As a result, the X-ray-detectable kinetic cubic α-$NaREF_4$ phases can be

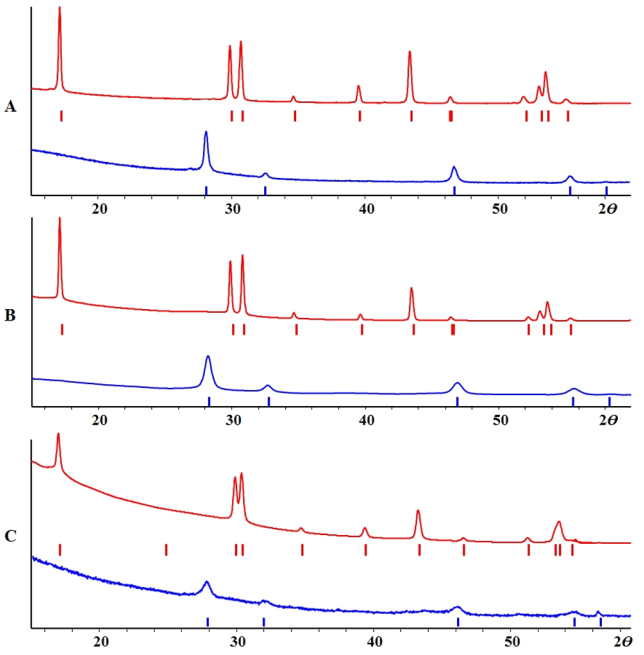

Figure 5. X-ray powder diffraction patterns of α-$NaREF_4$ (blue) and β-$NaREF_4$ (red) obtained by decomposition of $NaY(hfac)_4$ (A), $NaEr(hfac)_4$ (B), and $NaEu(hfac)_4$ (C) precursors under argon. Theoretical peak positions for α- and β-phases are shown as blue and red lines, respectively.

obtained at 225 °C/30 min (**1**), 325 °C/30 min (**2**), and 240 °C/24 h (**3**), while thermodynamic hexagonal β-$NaREF_4$ can be prepared at 575 °C/30 min (**1**), 475 °C/30 min (**2**), and 500 °C/30 min (**3**) (SI, Figures S19−S24). Unit cell parameters for $NaREF_4$ fluorides obtained by decomposition of

DOI: 10.1021/jacs.6b04194
J. Am. Chem. Soc. 2016, 138, 8883−8887

heterometallic precursors **1**−**3** match well to the literature data (Table 2).

Table 2. Comparison of Unit Cell Parameters for $NaREF_4$ Fluorides Obtained by Decomposition of $NaRE(hfac)_4$ (1−3) Precursors with the Literature Data

$NaREF_4$	space group	Le Bail fit results	literature data	ref
α-$NaYF_4$	$Fm\bar{3}m$	a = 5.4856(2)	a = 5.493(2)	20
β-$NaYF_4$	$P6_3/m$	a = 5.9763(1) c = 3.5208(1)	a = 5.991(5) c = 3.526(4)	20
α-$NaErF_4$	$Fm\bar{3}m$	a = 5.4752(9)	a = 5.465[a]	29
β-$NaErF_4$	$P\bar{6}$	a = 5.9747(2) c = 3.5023(1)	a = 5.959[a] c = 3.514[a]	30
α-$NaEuF_4$	$Fm\bar{3}m$	a = 5.597(1)	a = 5.603(1)	20
β-$NaEuF_4$	$P\bar{6}$	a = 6.0534(2) c = 3.6233(2)	a = 6.04(2) c = 3.62(1)	20

[a]No standard deviations reported.

Influence of annealing time on the formation of polymorph modifications at constant temperature has also been studied. Increasing the annealing time upon decomposition of $NaY(hfac)_4$ (**1**) precursor at 225 °C from 30 min (pure α-phase) leads to an appearance of the traces of β-modification after 12 h, and the latter became a major component after 48 h (Figure 6).

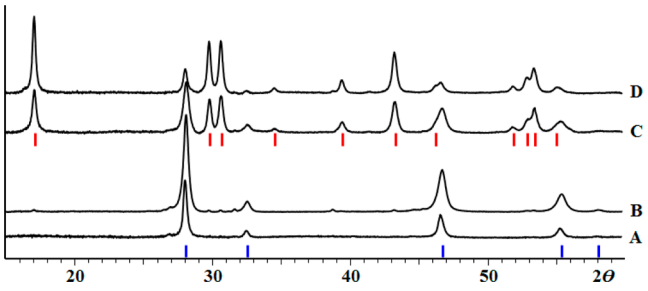

Figure 6. X-ray powder diffraction patterns of residues obtained by thermal decomposition of $NaY(hfac)_4$ (**1**) precursor under argon atmosphere at 225 °C with annealing times of 0.5 (A), 12 (B), 24 (C), and 48 (D) h. Theoretical peak positions for α- and β-$NaYF_4$ are shown as blue and red lines, respectively.

In conclusion, we report heterometallic precursors with fluorinated diketonate ligands $NaRE(hfac)_4$, where RE is either the principal element of a host matrix (Y) or the most common dopant (Er, Eu) for the corresponding $NaREF_4$ fluorides that are known as efficient up- and down-conversion materials. The title heterometallic compounds can be obtained by solution approach on a large scale, with high yield, using commercially available starting reagents. Highly volatile precursors feature heterometallic fragments in the gas phase and can be effectively utilized in the metal−organic chemical vapor deposition technique for thin-film growth due to a large temperature window between sublimation and decomposition. Thermolysis of fluorinated precursors in argon atmosphere was shown to yield phase-pure $NaREF_4$ materials. The low temperature of decomposition allows one to obtain both kinetic and thermodynamic polymorph modifications of the target fluorides. Importantly, the heterometallic diketonates are isomorphous and exhibit similar dimensions of the polymeric structures. The latter feature should be explored for a partial substitution of one rare earth metal for another in the process that may be dubbed as "precursor doping".

■ ASSOCIATED CONTENT

Supporting Information

The Supporting Information is available free of charge on the ACS Publications website at DOI: 10.1021/jacs.6b04194.

Full synthetic and characterization details; MS, IR, and NMR spectra; X-ray powder diffraction patterns; phase analysis of thermal decomposition products; and additional details on interatomic distances and angles in the structures of **1**−**3** (PDF)

X-ray crystallographic files for **1**−**3** (CIF)

■ AUTHOR INFORMATION

Corresponding Author

*edikarev@albany.edu

Notes

The authors declare no competing financial interest.

■ ACKNOWLEDGMENTS

Financial Support from the National Science Foundation CHE-1152441 (ED), CHE-1337594 (X-ray diffractometer), and CHE-1429329 (DART mass spectrometer) is gratefully acknowledged.

■ REFERENCES

(1) Kraemer, K. W.; Biner, D.; Frei, G.; Guedel, H. U.; Hehlen, M. P.; Luethi, S. R. *Chem. Mater.* **2004**, *16*, 1244−1251.

(2) (a) Singh, A. K.; Shahi, P. K.; Rai, S. B.; Ullrich, B. *RSC Adv.* **2015**, *5*, 16067−16073. (b) Guo, L.; Wang, Y.; Zou, Z.; Wang, B.; Guo, X.; Han, L.; Zeng, W. *J. Mater. Chem. C* **2014**, *2*, 2765−2772.

(3) Ramasamy, P.; Chandra, P.; Rhee, S. W.; Kim. *Nanoscale* **2013**, *5*, 8711−8717.

(4) (a) Luo, X. J.; Yuminami, R.; Sakurai, T.; Akimoto, K. *J. Phys.: Conf. Ser.* **2013**, *417*, 012054/1−012054/4. (b) Hao, X.-l.; Chen, Y.-s.; Chen, X.-p.; Zhou, J.-p.; Wang, H.-h.; Lu, J.-x.; Yang, S.-e. *J. Funct. Mater.* **2012**, *43*, 2286−2290.

(5) Stepuk, A.; Casola, G.; Schumacher, C. M.; Kramer, K. W.; Stark, W. J. *Chem. Mater.* **2014**, *26*, 2015−2020.

(6) (a) Li, C.; Lin, J. *J. Mater. Chem.* **2010**, *20*, 6831−6847. (b) Wang, Z.-L.; Chan, H. L. W.; Li, H.-L.; Hao, J. H. *Appl. Phys. Lett.* **2008**, *93*, 141106/1−141106/3.

(7) (a) Renero-Lecuna, C.; Martín-Rodríguez, R.; Valiente, R.; González, J.; Rodríguez, F.; Krämer, K. W.; Güdel, H. U. *Chem. Mater.* **2011**, *23* (15), 3442−3448. (b) Sommerdijk, J. L. *J. Lumin.* **1973**, *8*, 126−30. (c) Haase, M.; Schafer, H. *Angew. Chem., Int. Ed.* **2011**, *50*, 5808−29.

(8) (a) Fischer, S.; Froehlich, B.; Kraemer, K. W.; Goldschmidt, J. C. *J. Phys. Chem. C* **2014**, *118*, 30106−30114. (b) Shalav, A.; Richards, B. S.; Trupke, T.; Kramer, K. W.; Gudel, H. U. *Appl. Phys. Lett.* **2005**, *86*, 013505/1−013505/3. (c) Fischer, S.; Goldschmidt, J. C.; Loeper, P.; Bauer, G. H.; Brueggemann, R.; Kraemer, K.; Biner, D.; Hermle, M.; Glunz, S. W. *J. Appl. Phys.* **2010**, *108*, 044912/1−044912/11. (d) Chen, Y.; He, W.; Jiao, Y.; Wang, H.; Hao, X.; Lu, J.; Yang, S.-e. *J. Lumin.* **2012**, *132*, 2247−2250. (e) Cao, C.; Yang, H. K.; Chung, J. W.; Moon, B. K.; Choi, B. C.; Jeong, J. H.; Kim, K. H. *Mater. Res. Bull.* **2011**, *46*, 1553−1559. (f) Banski, M.; Afzaal, M.; Podhorodecki, A.; Misiewicz, J.; Abdelhady, A. L.; O'Brien, P. *J. Nanopart. Res.* **2012**, *14*, 1228/1−1228/10.

DOI: 10.1021/jacs.6b04194
J. Am. Chem. Soc. 2016, 138, 8883−8887

(9) (a) Zhao, J.; Sun, Y.; Kong, X.; Tian, L.; Wang, Y.; Tu, L.; Zhao, J.; Zhang, H. *J. Phys. Chem. B* **2008**, *112*, 15666−15672. (b) Thoma, R. E.; Hebert, G. M.; Insley, H.; Weaver, C. F. *Inorg. Chem.* **1963**, *2*, 1005−12. (c) Zhuang, J.; Yang, X.; Wang, J.; Lei, B.; Liu, Y.; Wu, M. *J. Solid State Chem.* **2016**, *233*, 178−185.
(10) Tu, D.; Liu, Y.; Zhu, H.; Li, R.; Liu, L.; Chen, X. *Angew. Chem., Int. Ed.* **2013**, *52*, 1128−1133.
(11) Cheng, W.; Zhang, J.-Z.; Xia, H.-P.; Feng, Z.-G.; Jiang, D.-S.; Jian, Z.; Gu, X.-M.; Zhang, J.-L.; Jiang, H.-C.; Chen, B.-J. *Optik (Munich, Ger.)* **2016**, *127*, 2608−2612.
(12) (a) He, M.; Pang, X.; Liu, X.; Jiang, B.; He, Y.; Snaith, H.; Lin, Z. *Angew. Chem., Int. Ed.* **2016**, *55*, 4280−4284. (b) Shao, B.; Feng, Y.; Song, Y.; Jiao, M.; Lu, W.; You, H. *Inorg. Chem.* **2016**, *55*, 1912−1919.
(13) (a) Lu, A.-H.; Salabas, E. L.; Schuth, F. *Angew. Chem., Int. Ed.* **2007**, *46*, 1222−44. (b) Shan, J.; Ju, Y. *Nanotechnology* **2009**, *20*, 275603/1−275603/13.
(14) (a) Ren, J.; Jia, G.; Guo, Y.; Wang, A.; Xu, S. *J. Phys. Chem. C* **2016**, *120*, 1342−1351. (b) Wang, L.; Yan, R.; Huo, Z.; Wang, L.; Zeng, J.; Bao, J.; Wang, X.; Peng, Q.; Li, Y. *Angew. Chem., Int. Ed.* **2005**, *44*, 6054−7.
(15) Yi, G.; Lu, H.; Zhao, S.; Ge, Y.; Yang, W.; Chen, D.; Guo, L.-H. *Nano Lett.* **2004**, *4*, 2191−2196.
(16) (a) Weingartner, H. *Angew. Chem., Int. Ed.* **2008**, *47*, 654−70. (b) Nunez, N. O.; Ocana, M. *Nanotechnology* **2007**, *18*, 455606/1−455606/7.
(17) Lin, C.; Berry, M. T.; Anderson, R.; Smith, S.; May, P. S. *Chem. Mater.* **2009**, *21*, 3406−3413.
(18) Wisser, M. D.; Chea, M.; Lin, Y.; Wu, D. M.; Mao, W. L.; Salleo, A.; Dionne, J. A. *Nano Lett.* **2015**, *15*, 1891−1897.
(19) Lee, H. I.; Pak, C.; Yi, S. H.; Shon, J. K.; Kim, S. S.; So, B. G.; Chang, H.; Yie, J. E.; Kwon, Y.-U.; Kim, J. M. *J. Mater. Chem.* **2005**, *15*, 4711−4717.
(20) Mai, H.-X.; Zhang, Y.-W.; Si, R.; Yan, Z.-G.; Sun, L.-d.; You, L.-P.; Yan, C.-H. *J. Am. Chem. Soc.* **2006**, *128*, 6426−6436.
(21) (a) Chen, X.; Peng, D.; Wang, F. *Nanomaterials* **2013**, *3*, 583−591. (b) Banski, M.; Podhorodecki, A.; Misiewicz, J. *Phys. Chem. Chem. Phys.* **2013**, *15*, 19232−19241.
(22) Huang, W.; Lu, C.; Jiang, C.; Wang, W.; Song, J.; Ni, Y.; Xu, Z. *J. Colloid Interface Sci.* **2012**, *376*, 34−39.
(23) (a) Zheng, K.; Song, W.; Lv, C.; Liu, Z.; Qin, W. *CrystEngComm* **2014**, *16*, 4329−4337. (b) Niu, N.; He, F.; Gai, S.; Li, C.; Zhang, X.; Huang, S.; Yang, P. *J. Mater. Chem.* **2012**, *22*, 21613−21623.
(24) Mishra, S.; Ledoux, G.; Jeanneau, E.; Daniele, S.; Joubert, M.-F. *Dalton Trans.* **2012**, *41*, 1490−1502.
(25) (a) Batsanov, S. S. *J. Mol. Struct.* **2011**, *990*, 63−66. (b) Bondi, A. *J. Phys. Chem.* **1964**, *68*, 441−51.
(26) (a) Bennett, M. J.; Cotton, F. A.; Legzdins, P.; Lippard, S. J. *Inorg. Chem.* **1968**, *7*, 1770−6. (b) Monguzzi, A.; Milani, A.; Mech, A.; Brambilla, L.; Tubino, R.; Castellano, C.; Demartin, F.; Meinardi, F.; Castiglioni, C. *Synth. Met.* **2012**, *161*, 2693−2699. (c) Burns, J. H.; Danford, M. D. *Inorg. Chem.* **1969**, *8*, 1780−1784.
(27) Dikarev, E. V.; Zhang, H.; Li, B. *J. Am. Chem. Soc.* **2005**, *127*, 6156−6157.
(28) (a) Wei, Z.; Filatov, A. S.; Dikarev, E. V. *J. Am. Chem. Soc.* **2013**, *135*, 12216−12219. (b) Navulla, A.; Huynh, L.; Wei, Z.; Filatov, A. S.; Dikarev, E. V. *J. Am. Chem. Soc.* **2012**, *134*, 5762−5765. (c) Lieberman, C. M.; Navulla, A.; Zhang, H.; Filatov, A. S.; Dikarev, E. V. *Inorg. Chem.* **2014**, *53*, 4733−4738. (d) Zhang, H.; Yang, J.-H.; Shpanchenko, R. V.; Abakumov, A. M.; Hadermann, J.; Clerac, R.; Dikarev, E. V. *Inorg. Chem.* **2009**, *48*, 8480−8488.
(29) Roy, D. M.; Roy, R. *J. Electrochem. Soc.* **1964**, *111*, 421−9.
(30) Brunton, G. D.; Insley, H.; McVay, T. N.; Thoma, R. E. *United States Atomic Energy Commission*; Oak Ridge National Laboratory: Oak Ridge, TN, 1965.

DOI: 10.1021/jacs.6b04194
J. Am. Chem. Soc. 2016, 138, 8883−8887